EVALUATION OF THE EFFECTS OF AN EL NIÑO EVENT ON GLACIER MELTING RATE

Freddy SORIA[1], So KAZAMA[2]

1 Member of JSCE, M. Eng., Graduate Student, Civil Engineering Dept., Tohoku University (Aobayama 6-6-06, Sendai, Japan)
2 Member of JSCE, D. Eng., Associate Professor, Graduate School of Environmental Studies, Tohoku University (Aobayama 6-6-06, Sendai, Japan)

The manuscript assumes the El Niño 1997-1998 event as the worst-case scenario for the estimation of probable effects on glacier melting rate due to the event 2009-2010. Evaluation is done at Zongo glacier (tropical Andes, Bolivia). The hydrograph is calculated for year 2008-2009 with the Snowmelt Runoff Model SRM, and the aid of Landsat imagery. A Gamma distribution is modified to estimate El Niño conditions. Resultant cumulative distributions show an increase of 35% in the peak rate for the period December-March, without implying a major frequency of peak flows. For November and April, the characteristics are similar, suggesting higher volumes, and less differences between high and low flows. Based on previous events, other months are assumed not affected by El Nino conditions.

Key Words **:** *Degree-day model, Landsat imagery, Gamma distribution.*

1. INTRODUCTION

Variations in glacier melting rates are important parameters to evaluate the effects of El Niño on water resources. Assessment for remote locations such as the Cordillera Real in the Tropical Andes is a task for which reliable records are often scarse[1), 2), 3)]. The objective of the manuscript is to apply the structure of the Snowmelt Runoff Model SRM[4)] to evaluate the effects that a strong El Niño event has on the melting rate of a glacierized catchment. For such purposes, conditions observed during the 1997-1998 El Niño event[5)] are assumed as the worst-case scenario towards the upcoming 2009-2010 El Niño event.

Daily observations during year 1999-2000[5)] are employed to calibrate the SRM, and to simulate the pre-El Niño year 2008-2009. Later, Gamma cumulative distribution functions CDF are employed to estimate the parameters of El Niño 2009-2010, based on observed conditions during the period 1997-1998[5)]. The final objective is to estimate seasonal CDF curves of glacier melt rate, through a bias correction technique[13)] that is applicable to regions with few data.

The glacier melting model employed is based on the temperature-index concept[4),6)], and remotely sensed glacier areal estimations[1), 7)]. The model assumes ablation correlated to air temperature more than it might be to net radiation[7), 8)] which makes the approach suitable to remote locations where air temperature records are the most readily available information. The applicability of the methodology is further beneficiated by the increasing amount of remotely sensed data released at no cost during the last decade, which increases the potential for the evaluation of regional effects[5), 9)].

2. BACKGROUND

(1) Study area and generalities

The study is on the Cordillera Real, western Bolivia (Fig.1), and the snowmelt estimation is done at the Zongo glacier (catchment area=3.46km^2), between -68.1 to -68.1W and -16.27 to -16.28S. The Cordillera divides the dry Altiplano (600 mm/year of precipitation) from the humid region of the headwaters of Amazon basin (2000 mm/year of precipitation). Glaciers in the study area are temperate[1)], with a wet snow zone and an ablation zone. The upper part of the wet zone is delimited by the *wet-snow line*, determined by snow from the last melt season whose temperature T is at melting point. Ablation season in the region continues throughout the year[1), 10)], with an integral role as reservoirs of water, and as sanctuaries that preserve endemic ecosystems.

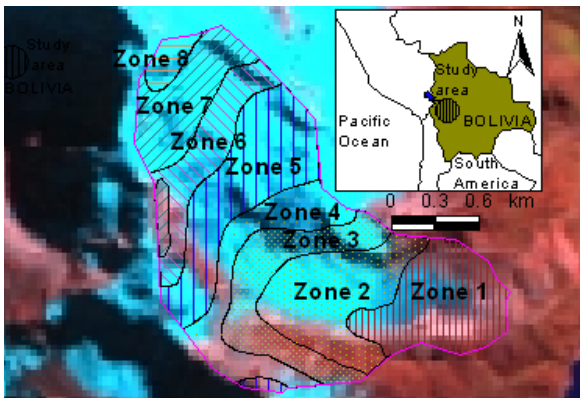

Fig.1 Study area, and zones considered in the SRM.

3. DATA

(1) Optical imagery and DEM data

Remotely sensing imagery have the advantage of monitoring wide and remote areas, hence are applicable to glacierized mountains[7), 4)]. Imagery from the Landsat platforms for the region is obtained at no cost from the archive released on January 2009 by the United States Geological Service USGS Earth Resources Observation and Science EROS (Table 1). Imagery is acquired from a Thematic Mapper TM instrument (30 m resolution and 6 bands), and the Enhanced Thematic Mapper ETM+ (with an improved resolution of the thermal band to 60 m from the 120m in the TM). The projection is the UTM–WGS84 system, GeoTIFF format, and cubic convolution resampling. The Level 1 Product Generation System (LPGS) processed data with Standard Terrain Correction (L1T), meaning systematic radiometric and geometric accuracy incorporated through ground control points from the SRTM DEM (Shuttle Radar Topography Mission Digital Elevation Model). ETM+ imagery acquired after July 14th, 2003 with the Scan Line Correction in off mode do not affect the study area. Landsat glacier areas are processed from short wavelength infrared false color composites[11)], with no pan-sharpening.

The DEM data source is the ASTER GDEM (Advanced Spaceborne Thermal Emission and Reflection Radiometer Global DEM), released on June 29th, 2009, and distributed by Japan's Ministry of Economy, Trade and Industry METI and NASA through the Earth Remote Sensing Data Analysis Center (ERSDAC) and the NASA Land Processes Distributed Active Archive Center (LP DAAC) at no cost. For a region in Bolivia to the south of the study area[12)], the mean difference ASTER–reference DEM = -10.9, with 8.1 m accuracy at 90% linear error confidence. The spatial detail resolvable by the GDEM is about 120m.

(2) Hydrometeorological observations

Available published data for Zongo glacier is: discharge Q, temperature T, and precipitation P, in a daily basis for years 1996-1997 and 1999-2000 (4830 masl)[1), 10)]; monthly Q at Zongo for the period 1991-2000[5)], monthly P at Plataforma[5), 9)] (4750masl) for 1991-2000, monthly P and T (1991-2000) and daily P and T (2008-2009) at El Alto (4000 masl).

Synthetic climatic data is used for the calculations, instead of using outputs from global circulation models because of the coarse resolution at which they are available. Trends observed at Zongo glacier (4830masl) in years 1996-1997 and 1999-2000 are employed to correct the bias of daily P in year 2008-2009 observed at El Alto station (4000masl). Bias correction of P is done based on a Gamma distribution[13)], and daily air temperatures at El Alto (4000masl) are bias corrected considering lapse rates[4)] from records of years 1996-1997 (at 5150masl) and 1999-2000 (at 4830masl).

4. SNOW AND ICE MELT MODELLING

The SRM[4)] is considered to evaluate the implications of El Niño event on glacier melting rate, assuming similarity to the worst-case scenario of the 1997-1998 event. For the modeling process the basin area is divided into accumulation, ablation, and ice-free area. Considering the glacier characteristics, Zongo glacier is subdivided in seven zones (Fig.1). The parameters are summarized in Table 2.

The model calculates runoff by addition of snow melt and glacier ice melt volumetric rates, and precipitation on snow and glacier free areas at each time period. The runoff is superimposed on the recession flow calculated, and transformed to discharge with Eq.1.

Table 1 Landsat imagery employed in the analysis.

Sensor ID	Acquisition date [year-month-day]	Product type
TM	1996-08-10 ; 1996-08-26 ; 1996-10-13 ; 1997-05-09 ; 1997-05-25 ; 1997-06-10 ; 1997-07-28 ; 1997-08-29 ; 1999-05-15 ; 1999-06-16 ; 1999-07-02 ; 1999-08-03 ; 2000-05-01 ; 2000-06-02 ; 2000-07-04 ; 2000-08-05 ; 2000-09-14; 2007-05-05 ; 2007-24-07	L1T
ETM+	2000-04-23 ; 2000-05-09 ; 2000-05-25 ; 2000-06-26 ; 2007-06-14 ; 2007-06-30 ; 2007-07-16 ; 2007-08-01 ; 2007-09-02 ; 2007-09-18 ; 2007-10-04 ; 2007-10-20 ; 2008-01-24 ; 2008-07-02	L1T

$$Q_n = C_n[P_n + a_n(T_n + \Delta T)S_n]A(1 - k_{n+1}) + Q_n k_{n+1} \quad (1)$$

where Q is the daily discharge [m^3/s], C is the runoff coefficient, a_n is the degree day factor [cm/(^oC day)], T is the number of degree days, ΔT is the temperature lapse rate correction factor when extrapolating the observations at a station, S is the ratio of snow-covered or glaciated area to the total area, P is the total daily precipitation [mm], A is the areal portion [km^2], k is the recession coefficient, n is the sequence of days. For Zongo glacier, the second term of Eq.1 where S is involved is composed by four terms: 1) a glacier-free portion covered by seasonal snow, 2) a glacier-free and snow-free portion, 3) a glacier portion covered by fresh snow, and 4) a glacier only portion[14)].

(1) Model parameters

a) Degree day factor *a*.

The *a* factor is estimated at the outlet of the basin from Eq.2, where ρ is density. Seasonally, $\rho_{ICE\ or\ SNOW}$ is varied according to the snow cover area observed on the corresponding Landsat imagery. Degree day factors are also varied in every zone according to variations in $\rho_{ICE\ or\ SNOW}$. Degree day factors are either varied from day to day, or averaged over 3 to 5 days, depending on the lag between temperature and melting[6)].

$$a = 1.1\frac{\rho_{SNOWorICE}}{\rho_{WATER}} \quad (2)$$

b) Temperature lapse rate correction factor ΔT.

The mean-along slope lapse rate is in average 0.49±0.03 ^oC/100 m. The rate is assigned to June, and assumed to follow seasonal trends drawn from the differences between the temperatures at El Alto and Zongo station for year 1999-2000. Eq.3 (where h is the elevation in meters) is employed to calculate the hypsographic distribution along the zones in the Zongo glacier.

$$\Delta T = \frac{LapseRate[^oC]}{100m}(h_{station} - h_{zone}) \quad (3)$$

c) The relationship ablation-air temperature

Ablation is correlated to air temperature more than it might be to net radiation[1)]. This provides a simple alternative for glacier melting, and is the basis of the considered approach.

d) Critical temperature T_{CRIT}

Observations over the period 1999-2000[1)] are taken to estimate T_{CRIT} by comparison between mean daily temperature, precipitation, discharge, and Landsat imagery when available. As a result, for June, July and August, monthly T_{CRIT} = mean maximum observed temperature = 1.2 ^oC, considering that during such period rainfall events fall as snow. That aspect is confirmed by Landsat imagery acquired in June 2nd 2000, and January 24th 2008. For other months values for T_{CRIT} are drawn by manual calibration of model outputs.

e) Depletion curve.

Curves are constructed from Landsat imagery, by replacing "time" with "cumulative snowmelt depths" in the x axis (i.e. the so called modified depletion curves[4)]). Information for inexistent or cloud covered scenes are estimated by linear interpolation from usable Landsat imagery. Thus, for the year 2008-2009, imagery available for the closest year is employed (2007-2008), and linear extrapolation is considered to extend the series.

f) Lag time.

Daily records for the period 1999-2000[1)] are employed to estimate time lags between the input (temperature) and the output (melting rate). Thus, 4 days are assigned to September and October. For other months time lag is initially calibrated (Table 2), but finally disregarded.

g) Runoff coefficient C.

C is the ratio between total monthly rainfall or snow and the discharge. For the whole glacier, observations for the year 1999-2000[1)] are used to calculate Cs and Cr, i.e. for snow and rain respectively. Initial estimations assume Cs 80% lower than Cr, considering that the glacier is on a granite formation[1)], and loses are expected in the zones 1 to 3 where moraines develop. Final values in Table 2 are result of calibration.

h) Recession coefficient k.

Parameter k is seasonally distributed from daily records in year 1999-2000. k is the rate Q_{n+1} to Q_n, and is commonly calculated from recession plots[4)]. In our work, k_x and k_y in Eq.4 are estimated from historical records of air temperature series, which is considered the most influential model parameter. This consideration also allows reducing the number of parameters to calibrate.

$$k_{n+1} = k_x Q_n^{-ky} \quad (4)$$

i) Model accuracy.

Multiple statistical measures are employed for model performance evaluation. Measures are based on a normalized form of squared residuals (differences between observed Ot and computed data Ct) and ordinary error measures to emphasize the performance during high flows and evaluate concordance with observations respectively. Nash-Sutcliffe dimensionless Coefficient of Efficiency (CE) varies from minus infinity, for poor model performance, to 1.0 for good model performance

Table 2 Summary of parameters employed in the calibration.

Parameter	Zone	sep	oct	nov	dec	jan	feb	mar	apr	may	jun	jul	aug
a [cm/°C month]	Zone 1	0.91	0.93	0.74	0.96	0.82	0.96	0.96	0.96	0.94	0.90	0.85	0.88
	Zone 2	0.90	0.88	0.70	0.96	0.69	0.73	0.96	0.96	0.91	0.89	0.82	0.90
	Zone 3	0.61	0.63	0.31	0.77	0.58	0.29	0.77	0.36	0.61	0.65	0.65	0.73
	Zone 4	0.65	0.46	0.37	0.77	0.50	0.35	0.22	0.58	0.65	0.74	0.61	0.65
	Zone 5	0.43	0.43	0.35	0.44	0.44	0.24	0.07	0.31	0.42	0.44	0.38	0.40
	Zone 6	0.32	0.35	0.25	0.28	0.33	0.26	0.12	0.34	0.33	0.29	0.29	0.31
	Zone 7	0.28	0.28	0.22	0.28	0.28	0.28	0.28	0.28	0.28	0.28	0.28	0.28
T_{CRIT} [°C]	All zones	0	0.5	0.8	0.8	1	1.2	1.2	1	1	1	1	1
Lapse rate [°C/100 m]	All zones	0.59	0.60	0.69	0.76	0.76	0.81	0.65	0.60	0.48	0.49	0.40	0.58
Time lag [days]	All zones	5	5	2	2	0	2	1	1	1	1	1	1
Cr	All zones	0.80	0.90	0.85	0.70	0.80	0.67	0.57	0.70	0.80	0.90	0.95	0.95
Cs	All zones	0.80	0.90	0.85	0.85	0.85	0.85	0.85	0.75	0.80	0.95	0.90	0.90
k_y	Basin outlet	-0.140	-0.174	-0.063	-0.066	-0.033	-0.046	-0.014	-0.055	-0.034	-0.051	-0.207	-0.291
k_x	Basin outlet	0.663	0.682	0.844	0.846	0.925	0.863	0.855	0.857	0.835	0.816	0.658	0.559

(Eq.5). The dimensionless Relative Volumetric Error (RVE) evaluates volumetric concordance between the calculated and the observed series (Eq.6).

$$CE = 1 - \frac{\sum (O_t - C_t)^2}{\sum (O_t - O_{mean})^2} \qquad (5)$$

$$RVE = \frac{\sum (O_t - C_t)}{\sum O_t} \qquad (6)$$

5. RESULTS

(1) Effect of the 1997-1998 El Niño on catchment runoff

Historical monthly records of P and Q[5] show that the event increased average yearly Q in the catchment in about 55% respect to the average of years 1996-1997 and 1999-2000, and about 40% respect to the Q averaged over the period showed in Fig.2. The effect is not due to precipitation, but to the increase in yearly average temperatures (see the T anomalies at El Alto in Fig.2). Effects on other variables are reported in published manuscriots[5], and are out of the scope of the current paper.

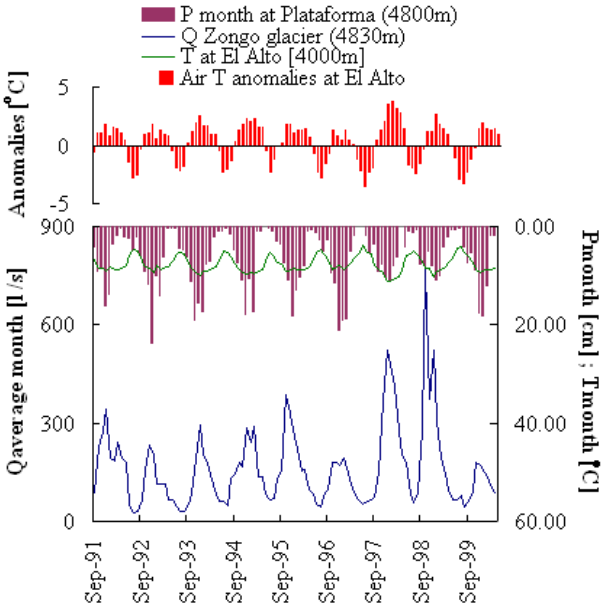

Fig.2 Monthly response of the Zongo basin, and temperature anomalies respect to the base period 1960-1990.

(2) Model calibration

Observations for year 1999-2000[1] are used to calibrate the structure of the SRM model, and the results are shown in Fig.3. One at a time experiments[15] evaluate model sensitivity, where the most influential parameter is k, followed by the degree days, C, and S. The model performance is adequate since the objective is the overall volumetric concordance (CE=0.55, and RVE=0.0217m^3/s), due to its importance in water resources availability. Time lag between degree days and glacier melting decrease as the hydrograph

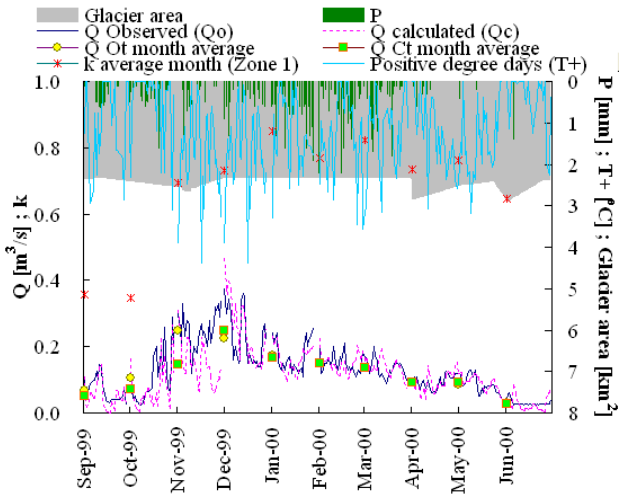

Fig.3 Model calibration for year 1999-2000.

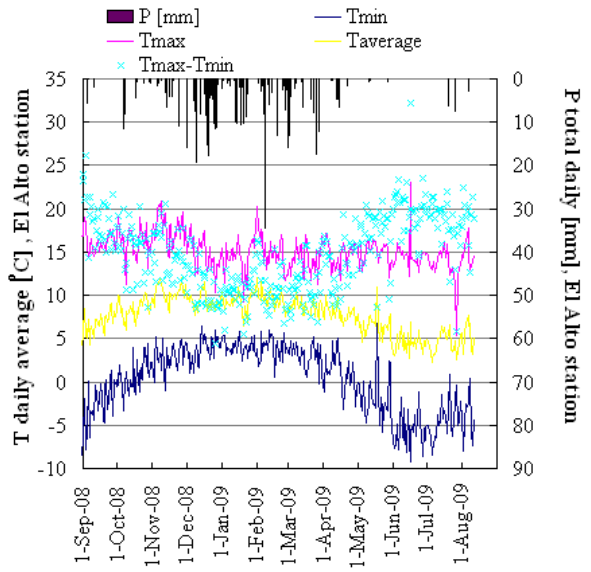

Fig.4 Seasonal variation of climatic variables at El Alto station.

trend rises. During September precipitation falls as snow and the number of positive degree days[6] are integrated over 4 days. In October a similar criterion is considered, improving the model performance only during the peaks. Degree days increase together with glacier melt rates, with high variations from day to day (i.e. high values of recession constants, Fig.3). In November the lag between Q and T decreases, and the calculation demands degree days integrated over variable time intervals. At that time the solution found for hydrograph concordance in September is no longer applied, due to a lack of an appropriate criterion for integrating the number of degree days at variable intervals. In December glacier melt reaches the highest rates, and shows high correlation T-Q, resulting in a good model performance. The first melting period finishes around January, coincident with the period with the highest temperatures; at the same time the hydrograph starts receding. From then until March, P rates increase, causing T and Q to fall (monthly trends of the Q stabilize), and glacier ablation is "controlled". Positive degree days indicate that ablation continues towards May, with the presence of isolated snow events.

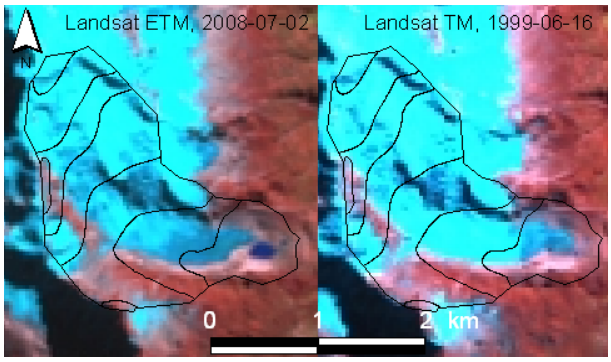

Fig.5 Glacier retreat as seen from Landsat platform.

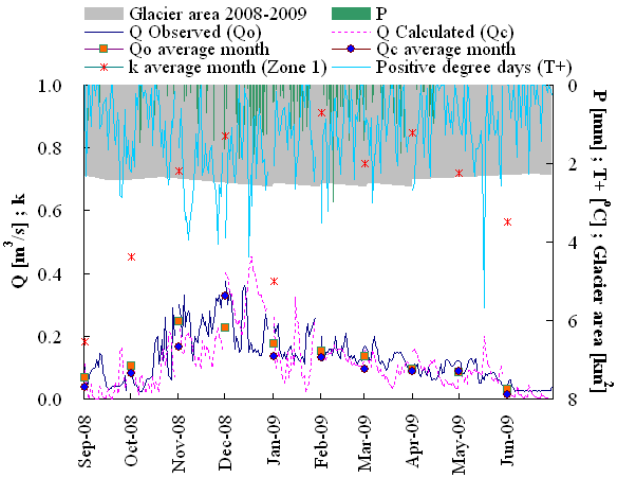

Fig.6 Model simulation for year 2008-2009.

Melting during winter is particularly interesting. It has low sensitivity to the number of degree days, despite that in the region is common to observe high maximum temperatures (Tmax) during day hours (see Fig.4). For this period the calculation is aimed to estimate the volumetric concordance and the results are satisfactory. Besides the considerations above, simulations for future years are affected by the melted glacier portion at the tongue that form a glacial lake (Fig. 5), which further buffers the peaks, and increases the lag between T and Q.

(3) Glacier melting for year 2008-2009

The glacier melting hydrograph for year 2008-2009 is calculated employing the parameter values of the 1999-2000 simulation (Fig. 6). Comparison of CDFs indicate that years 1996-1997 and 1999-2000 are similar (Fig.7), therefore the calibration selected for only one of them is justified.

The glacial lake in Fig 5 increases the T-Q lag, and is incorporated in the simulation by considering positive degree days integrated over 5 days for

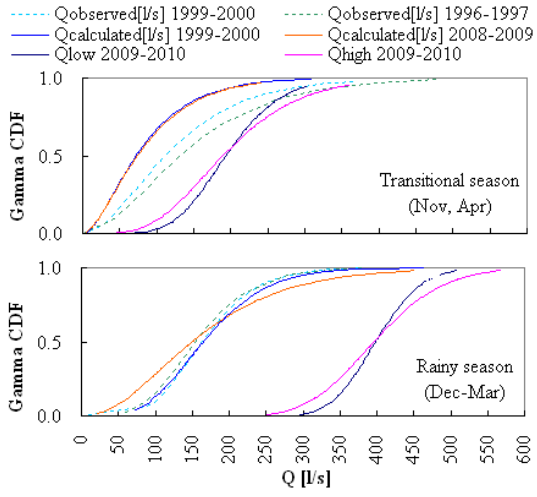

Fig.7 Comparison of Gamma CDF, where Qlow is the CDF with lowest standard deviation, and Qhigh is the opposite.

September and October (1 day more longer than the 1999-2000 simulation). For the remaining months the integration is not considered because there is a lack of adequate criterion for defining the irregular behavior in time.

The first Gamma CDF parameter μ for the 2009-2010 event is the average monthly discharge during El Niño year 1997-1998, and the second Gamma CDF parameter are standard deviations σ within a range that keeps the CDF under behavioral boundaries. Fig.7 compares CDFs for "normal" years, and those generated for El Niño event. During rainy season, Gamma CDFs with μ=400 l/s and σ=50 l/s to 75 l/s, draw daily flow rates that vary from 250 l/s to 290 l/s until peaks of 600 l/s (35% over the highest peak in December). During the transitional season, Gamma CDFs with μ=200 l/s and σ=50 l/s to 75 l/s, draw daily flow rates that vary from 12 l/s to 40 l/s until peaks of 360 l/s, without departing much from the simulation, but with steeped CDF configuration that ensures more frequent high flows. El Niño 1997-1998 does not affect considerably mean values of remaining months, therefore are not shown.

5. CONCLUSIONS

Through this approach was pretend to apply a methodology that includes the least number of parameters, in order to facilitate its use in remote locations. It is also aimed to estimate potential El Niño conditions based on the characteristics of an El Niña year, in order to not overestimate the results. Despite our intentions, the results present CDFs with large departure from common observations recorded. The impact of El Niño event causes high variability of the melting rate during hydrograph rise, which is represented by the steepness of the CDFs estimated. Nevertheless, sharp hydrograph rise would not cause significant damage due to the magnitude of the discharge, but would be a potential threat in case of avalanches. During rainy season was interesting to observe that considering 400 l/s as observed monthly average, the Gamma CDF showed peaks of 600 l/s as maximum values, and a significant departure from a normal year. As mentioned, melting rates may not represent a threat to civil infrastructure, but do represent a threat to the equilibrium state of the glaciers, and would constitute a threat for the management of the Zongo reservoir that feds the main hydropower system for the city of La Paz. The necessity of regionalizing the results towards ungauged locations remain, and is aimed to be covered in upcoming publications.

ACKNOWLEDGMENT: The authors wish to thank to the Glacier Retreat Impact Assessment and National Policy Development (GRANDE), under the Science and Technology Research Partnership for Sustainable Development (SATREPS), for kindly providing part of the records.

REFERENCES

1) Sicart, J., Ribstein, P., Francou, B., Pouyaud, B., Condom, T.: Glacier mass balance of tropical Zongo glacier, Bolivia, comparing hydrological and glaciological methods, *Global Planet. Change*, Vol. 59, pp.27–36, 2007.
2) Schaefli, B., Hingray, B., Niggli, M., Musy, A.: A conceptual glacio-hydrological model for high mountainous catchments, *Hydrol.Earth Syst.Sci.*, Vol.9, pp.95–109, 2005.
3) Vimeux, F., Gallaire, R., Bony, S., Hoffmann, G., Chiang, J.: What are the climate controls on δD in precipitation in the Zongo Valley (Bolivia)? Implications for the Illimani ice core interpretation, *Earth Planet. Sc. Let*, Vol. 240, pp. 205– 220, 2005.
4) Martinec, J., Rango, A., Roberts R.: *Snowmelt Runoff Model (SRM) User's Manual*, Gómez, E., Bleiweiss, M. eds., New Mexico State University, New Mexico, 2008.
5) Wagnon, P., Ribstein, P., Francou, B., Sicart, J.: Anomalous heat and mass budget on glaciar Zongo Bolivia, during the 1997-1998 El Niño year, *J. Glaciol.*, Vol. 47 (156), 2001.
6) Hock, R.: Temperature index melt modelling in mountain areas, *J. Hydrol.* Vol.282 pp.104–115, 2005.
7) Bamber, J. and Rivera, A.: A review of remote sensing methods for glacier mass balance determination, *Global Planet. Change*, Vol.59, pp.138-148, 2007.
8) Paterson, W.: *The physics of glaciers*, 3rd ed., Elsevier Science, Birlington, 1994.
9) Ramírez, E., Olmos, C., Román, A.: Melting of the Tuni Condoriri basin and its impact on the water resources of La Paz and El Alto cities (In Spanish), *Programa.de Investigación GRANT–GREAT ICE, IHH-IRD - Plan Quinquenal PNCC (Unpublished)*, 2007.
10) Wagnon, P., Ribstein, P., Francou, B., Pouyaud, B.: Annual cycle of energy balance of Zongo Glacier, Cordillera Real, Bolivia, *J. Geophys. Res.*, Vol. 104 (D4), pp. 3907-3923, 1999.
11) Soria, F., Kazama, S. : Evaluation Of Climate Change Effects On Glacier Area And Vegetation Using Remote Sensing Imagery, *Proc. 7th ISE Symp., Chile, 2009.*
12) METI/ERSDAC, NASA/LPDAAC, USGS/EROSASTER (the Global DEM Validation Team GDVT): Global DEM Validation-Summary Report, 2009.
13) Ines A, Hansen J.: Bias correction of daily GCM rainfall for crop simulation studies, *Agric. Forest Met.* Vol. 138, pp.44–53, 2006.
14) Schaper, S., Seidel, K., Martinec, J.: Precision snow cover and glacier mapping for runoff modelling in a high alpine basin, *Proc. of the Santa Fe Symp.*, IAHS Publ, 2000.
15) Saltelli A.: Sensitivity analysis for importance assessment. *Risk Analysis*, Vol. 22 (3), pp.579, 2002.

(Received September 30, 2009)